Journal of Colloid and Interface Science 362 (2011) 194–201

Contents lists available at ScienceDirect

Journal of Colloid and Interface Science

www.elsevier.com/locate/jcis

Impedimetric biosensor based on self-assembled hybrid cystein-gold nanoparticles and CramoLL lectin for bacterial lipopolysaccharide recognition

Maria D.L. Oliveira [a,*], Cesar A.S. Andrade [b], Maria T.S. Correia [a], Luana C.B.B. Coelho [a], Pankaj R. Singh [c], Xiangqun Zeng [c]

[a] Departamento de Bioquímica, Universidade Federal de Pernambuco-UFPE, 50670-901 Recife, PE, Brazil
[b] Centro Acadêmico de Vitória, Universidade Federal de Pernambuco, 55608-680 Vitória de Santo Antão, PE, Brazil
[c] Department of Chemistry, Oakland University, 2200 Squirrel Road, Rochester, MI 48309, USA

ARTICLE INFO

Article history:
Received 27 April 2011
Accepted 16 June 2011
Available online 24 June 2011

Keywords:
Impedance spectroscopy
Cyclic voltammetry
Bacterial lipopolysaccharide
Endotoxins
Cratylia mollis
Nanoparticles

ABSTRACT

We report the development of a new selective and specific electrochemical biosensor for bacterial lipopolysaccharide (LPS). An electrode interface was constructed using a L-cysteine-gold nanoparticle (AuNpCys) composite to be immobilized by electrostatic interaction in the network of a poly(vinyl chloride-vinyl acetate maleic acid) (PVM) layer on a gold bare electrode. The impedimetric biosensor is fabricated by self-assembled CramoLL lectin on the PVM–AuNpCys–modified gold electrode through electrostatic interaction. CramoLL is used as the recognition interface. AFM images showed that LPS was specifically recognized on the PVM–AuNpCys–CramoLL system surface. The measurements of cyclic voltammetry (CV) and electrochemical impedance spectroscopy (EIS) showed that the electrochemical response of a redox probe system ($K_4[Fe(CN)_6]^{4-}/K_3[Fe(CN)_6]^{3-}$) were blocked, due to the procedures of modified electrode with PVM–AuNpCys–CramoLL. In the majority of the experiments the lectin retained its activity as observed through its interaction with LPS from *Escherichia coli*, *Serratia marcescens*, *Salmonella enterica* and *Klebsiella pneumoniae*. The results are expressed in terms of the charge transfer resistance and current peak anodic using the EIS and CV techniques for the development of a biosensor for contamination by endotoxins. A new type of sensor for selective discrimination of LPS types with a high sensitivity has been obtained.

1. Introduction

In the past few years, there has been increasingly interest in obtaining new biodevices for the rapid detection of lipopolysaccharides (LPS), since they are common pathogens particularly in humans, animals and plants. LPS, also known as endotoxins, are the major surface-exposed structural component of the outer membrane of gram-negative bacteria [1] and are composed of three distinct regions: lipid A, core oligosaccharide, and O-specific antigen. The O-specific chain is an antigenic polysaccharide composed of a chain of highly variable repeating oligosaccharide subunits, typically three to six monosaccharide residues. The effects of endotoxin exposure on humans include fever, diarrhea, vomiting, septic shock, and disseminated intravascular coagulation [2]. In addition, the detection of bacterial LPS from strains of *Klebsiella pneumonia*, *Serratia marcescens*, *Escherichia coli* and *Salmonella enterica* plays an important role in research, industry, food control, public health and biodefense.

The LPS molecule is a virulence determinant in *K. pneumonia* and its aggregation with capsular polysaccharide has been implicated in tissue damage that typically results from active *K. pneumoniae* lobar pneumonia [3]. *Klebsiella* O antigens are composed of two discrete repeat-unit structures of D-galactan [4,5]. *S. marcescens* is an opportunistic pathogen and its endotoxins can cause endocarditis, meningitis, urinary tract infections and bloodstream infections [6]. LPS from *S. marcescens* exhibit a linear polysaccharide composed of D-glucose-L-rhamnose disaccharide [7]. *E. coli* is the most common pathogen associated with urinary tract infections (UTIs) in women, and accounts for 70–90% of community-acquired infections [8]. In addition, LPS from *E. coli* K-235 showed that the repetitive subunit sugar residues consist of glucosamine, galactosamine, glucose, galactose, rhamnose [9]. *S. enterica* remains a major cause of foodborne gastroenteritis worldwide. Many cases of human salmonellosis are attributed to the consumption of infected poultry, meat and eggs, the vast majority of cases being the result of *S. enterica* serovar *Enteritidis* or serovar *Typhimurium* [10]. LPS from *S. enterica* contain around 20 repeats of a common main-chain trisaccharide unit consisting of D-mannose, L-rhamnose, and D-galactose [11].

Currently, biotechnology is being used to produce diverse important pharmaceutical products by means of protein technologies,

* Corresponding author. Fax: +55 81 2126 8540.
E-mail address: m_danielly@yahoo.com.br (M.D.L. Oliveira).

0021-9797/$ - see front matter © 2011 Elsevier Inc. All rights reserved.
doi:10.1016/j.jcis.2011.06.042

recombinant DNA and/or fermentation from bacterial cells. In addition, the resulting pharmaceutical products are contaminated with LPS that are released from the host cells. LPS must therefore be removed from pharmaceutical products that are administered intravenously, such as infusion fluids and injections [12].

In addition, the presence of LPS in organisms results in a wide variety of biological effects such as septic shock and coagulopathies in humans. These biological effects result in disseminated intravascular coagulation, acute septicemic disease and multi-organ failure [2]. Thus, to ensure the quality of pharmaceuticals new methods are required to measure the LPS content [13]. Nowadays, there are three commonly available methods (chromogenic assay, gel-clot assay and kinetic turbidimetric assay) for LPS detection based on the Limulus lectin derived from the American horseshoe crab, known as Limulus amebocyte lysate (LAL) tests. New technologies such as LAL tests are therefore very sensitive, but are expensive and the time taken by the analysis is very long. Recently, Hreniak et al. [14] have used optodes to obtain a luminescence endotoxin biosensor, prepared by the sol–gel method, using a luminophor covalently attached to Concanavalin James et al. [15] developed a method to detect LPS from *E. coli* using fluorescent tapered fiber-optic biosensors based on the competitive assay. Polymyxin B (PMB) covalently immobilized onto the surface of the probe was used as a recognition molecule. Other authors [16] have also used PMB with quartz crystal microbalance (QCM) for the detection of endotoxin. PMB has been immobilized on the self-assembled monolayer-modified 10 MHz AT-cut quartz crystal resonator. However, prior to PMB immobilization, chemical modifications of the electrode were necessary. The self-assembled monolayers were activated with 1-[3-(dimethylamino)propyl]-3-ethylcarbodiimide hydrochloride and N-hydroxysuccinimide prior to PMB immobilization.

New methods for label-free detection of bacterial LPS with high accuracy, low cost and less processing time are generally involved in the use of lectins, a class of proteins which exhibit a specific affinity to carbohydrate moieties. We therefore exploited this binding characteristic to recognize sugar residues as a basis for the biosensor design for different bacteria. In this work we applied a self-assembly technology to develop a rapid and sensitive electrochemical biosensor for the detection of bacterial LPS from *S. enterica* serovar *Typhimurium*, *K. pneumonia*, *S. marcescens* and *E. coli* using a new lectin isolated from Cratylia mollis seeds as a selective recognition element. CramoLL is a lectin isolated from Cratylia mollis seeds [17] of the Leguminosae family and Dioclinae subtribe that recognizes Gly/Man and glycoproteins [18]. CramoLL is involved in many biological activities, such as antitumor action [19], and its specificity is correlated with the Concanavalin A lectin. CramoLL has monosaccharide binding sites with hydrogen bond interactions between protein and methyl-α-D-mannoside (MeαMan). One molecule of MeαMan in the monosaccharide binding site interacts through direct hydrogen bonds with Asn14, Leu99, Tyr100, Asp207, and Arg227 and through hydrophobic contacts with the side chains of Tyr12, Leu99, and Tyr100 [20].

As shown in Fig. 1, an electrode surface based on the poly(vinyl chloride-co-vinyl acetate-co-maleic acid) (PVM) with high a negative surface charge and affinity for cysteine-coated gold nanoparticles (AuNpCys) was firstly formed on a substrate electrode. PVM was selected based on its physical–chemical properties, good adhesion to the electrode surface and mainly its negative charge that improves the interaction process with CramoLL lectin by electrostatic interaction. In addition, AuNPs have a high surface-to-volume ratio and high surface energy to provide a stable immobilization of a large amount of biomolecules, retaining their bioactivity. Moreover, AuNPs have the ability to permit fast and direct electron transfer between a wide range of electroactive species and electrode materials. The deposition of PVM on the electrode surface formed a film with a large surface area for the assembly of AuNpCys and further immobilization of CramoLL lectin. Subsequently, the AuNpCys inorganic–organic composite containing an amine group with a positive charge was adsorbed on a negatively-charged PVM–modified gold electrode. Finally, negatively-charged CramoLL was immobilized on the AuNpCys–PVM composite film based on an electrostatic interaction between oppositely charged species (Fig. 1).

The stepwise assembly process of the biosensor was characterized by means of atomic force microscopy (AFM), cyclic voltammetry (CV) and electrochemical impedance spectroscopy (EIS). Assay conditions that were optimized included the incubation time of PVM–AuNpCys–CramoLL, and concentration and incubation time of the bacterial LPS recognition. Under optimal conditions, the biosensor response to LPS presented good accuracy, stability, and reproducibility. To our best knowledge, we have shown for the first time that CramoLL can be applied to the development of electrochemical biosensors for detecting LPS.

2. Materials and methods

2.1. Materials

CramoLL was obtained from the Laboratory of Glycoproteins (UFPE) [17]. Bovine serum albumin (BSA), L-cystein, potassium ferricyanide and LPS from *S. enterica* serotype *typhimurium* (strain ATCC7823), *K. pneumonia* (strain ATCC15380), *S. marcescens* (strain ATCC21639) and *E. coli* (strain ATCC13027) were purchased from Sigma Chemical (St. Louis, MO, USA). Potassium ferrocyanide was obtained from Merck. The AuNPs (mean size: 15 nm) were purchased from Ted Pella Inc. Poly-(vinyl chloride-co-vinyl acetate-co-maleic acid) (Polysciences, Inc.) consisting of 83% vinyl chloride, 13% vinyl acetate and 1% carboxylated of the respective monomers was used as provided in powder form without further purification or drying. Phosphate buffer saline (PBS) pH 7.2 was purchased from Gibco. All chemicals and solvents were of analytical grade and they were used as received, without further purification.

2.2. Preparation of AuNpCys nanocomposites

Hybrid AuNpCys composites were obtained according to Li et al. [21]. The preparation of AuNpCys was performed with 25 μL L-cysteine solution (10^{-3} M) self-assembled with 450 μL of AuNp for 12 h.

2.3. Electrode surface modification

The gold electrode surface was freshly polished prior to use with 0.05 μm α-Al_2O_3 paste, and rigorously rinsed with doubly distilled water following each polish. The polished electrode was then sequentially cleaned ultrasonically in water for 5 min. Initially, a 5 μL of PVM (0.2%) solution was coated onto the pretreated electrode and dried in air for 5 min, following which the electrode was dipped into AuNpCys solution for 30 min. Subsequently, it was rinsed with buffer and 5 μL of CramoLL solution (1.30 mg/mL) was dripped. The PVM–AuNpCys–CramoLL-modified electrode was incubated in a PBS solution containing 0.2% BSA for 20 min at 25 °C in order to block the remaining active sites. Finally, the resulting PVM–AuNpCys–CramoLL–BSA electrode was exposed to LPSs from *S. enterica*, *K. pneumoniae*, *S. marcescens* and *E. coli* at different concentrations (200 μg/mL, 150 μg/mL, 100 μg/mL, 50 μg/mL and 25 μg/mL) diluted in 10 mM pH 7.4 PBS solution at room temperature.

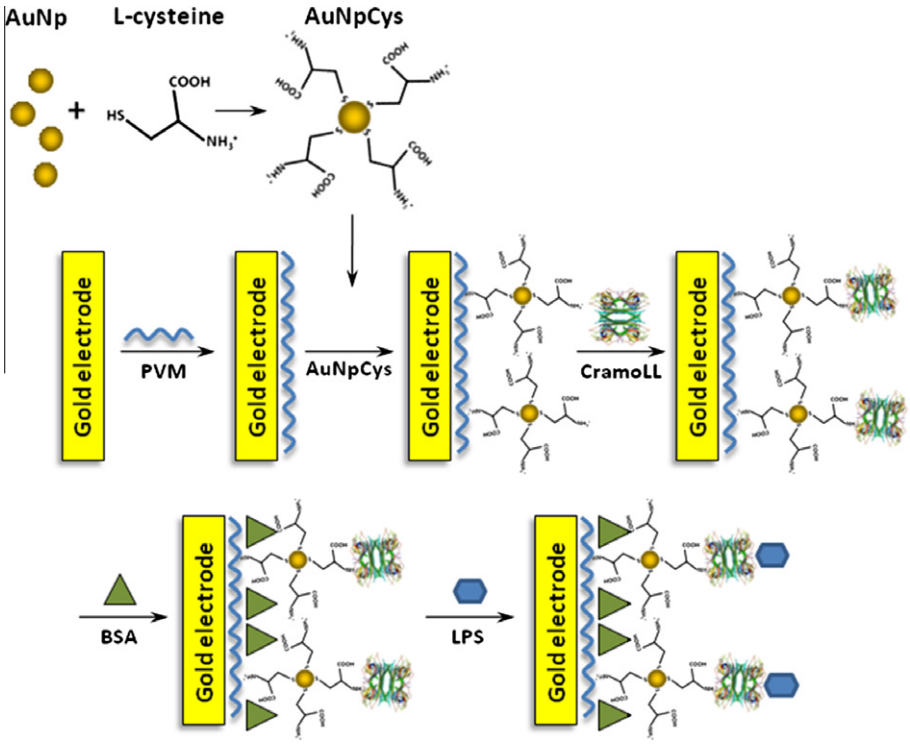

Fig. 1. Mechanism for the reaction of Cys with AuNp and schematic representation of the PVM–AuNpCys–CramoLL–BSA–LPS biosensor system.

2.4. Atomic force microscopy measurements

Atomic force microscopy (AFM) measurements were performed with a commercial PicoPlus microscope (Molecular Imaging, USA). Cantilevers with a Cr–Au tip (NSC18, MikroMasch, F_0 = 90 KHz, nominal spring constant = 5.5 N m^{-1}) were used for the tapping mode AFM in air at room temperature (approximately 25 °C) [22]. Scan areas with a resolution of 512 × 512 pixels were obtained, ranging from 1.0 μm × 1.0 μm. To eliminate artifacts, images were obtained from at least two macroscopically-separated areas on each sample.

2.5. Electrochemical measurements

Electrochemical measurements were carried out on a PARSTAT 2263 (Princeton Applied Research, USA) potentiostat controlled by a computer. The impedance spectra were recorded in the frequency range of 100 mHz to 100 kHz. All tests were conducted on an open circuit potential, and a single modulated AC potential of 10 mV was applied for impedance measurement. Cyclic voltammetric measurements were performed in a conventional electrochemical cell containing a three-electrode system and swept the potential between −0.3 and +0.7 V with a scan rate of 80 mV s^{-1} in a pH 7.4 PBS solution. Impedance measurement was performed in the presence of a 10 mM $K_4[Fe(CN)_6]^{4-}/K_3[Fe(CN)_6]^{3-}$ (1:1) mixture as a redox probe in a 10 mM PBS solution containing 0.1 M KCl [23,24]. All electrochemical measurements were performed at room temperature.

3. Results and discussion

3.1. UV–Vis measurements

Fig. S1 (see supporting information) shows the UV–Vis spectra of the AuNp and AuNpCys solutions. The strong absorption in the spectra of AuNp at 512 nm is the characteristic feature of Au plasmon resonance [25]. A bathochromic shift and broadening of the absorption band was obtained in the spectra of AuNpCys, indicating some aggregation to surface modification of AuNp. In addition, we observed a color change in the AuNp solution from pink–red to blue by the addition of Cys, indicating the interaction with AuNp.

3.2. AFM analysis

The morphology of the different steps of the multilayer assembly was analyzed by high-resolution *in situ* AFM imaging measurements. The AuNp are homogenously distributed on the HOPG surface, while the size of the nanoparticles is about 15 nm (Fig. 2a). We used HOPG as a substrate for imaging as it is atomic flat so that the assembled biointerface properties can be clearly observed. PVM forms a continuous and smooth layer on HOPG substrates (Fig. 2b). As shown in Fig. 2c, the AuNpCys particles formed were in the range of a few nanometers, which results in a large surface area and easier attachment of CramoLL molecules. The HOPG surfaces were functionalized with an AuNpCys–PVM monolayer on which CramoLL lectin was electrostatically adsorbed. Images of PVM–AuNpCys–CramoLL–BSA exhibit morphology with globular features ascribed to the AuNpCys and homogeneously distributed over the PVM surface (Fig. 2d). From the AFM image analysis the height of the PVM–AuNpCys–CramoLL–BSA system layer was determined to be around 24 nm.

LPS from *S. marcescens* molecules were adsorbed onto the PVM–AuNpCys–CramoLL–BSA system as an aggregated pattern in solid-like state and height about 34 nm (Fig. 2e). AFM images for LPS from *E. coli* (Fig. 2f) and *S. enterica* (Fig. 2g) indicated homogeneous films. The PVM–AuNpCys–CramoLL–BSA–*pneumoniae* shows a porous structure, and the height of the formed LPS layer is about 22 nm (Fig. 2h). With respect to the vertical dimensions, the differences between the relative rough profiles of the PVM–AuNpCys–CramoLL–BSA–LPS systems may be due to the differences in LPS lengths [26] and may result in the change in the electrochemical biosensor response.

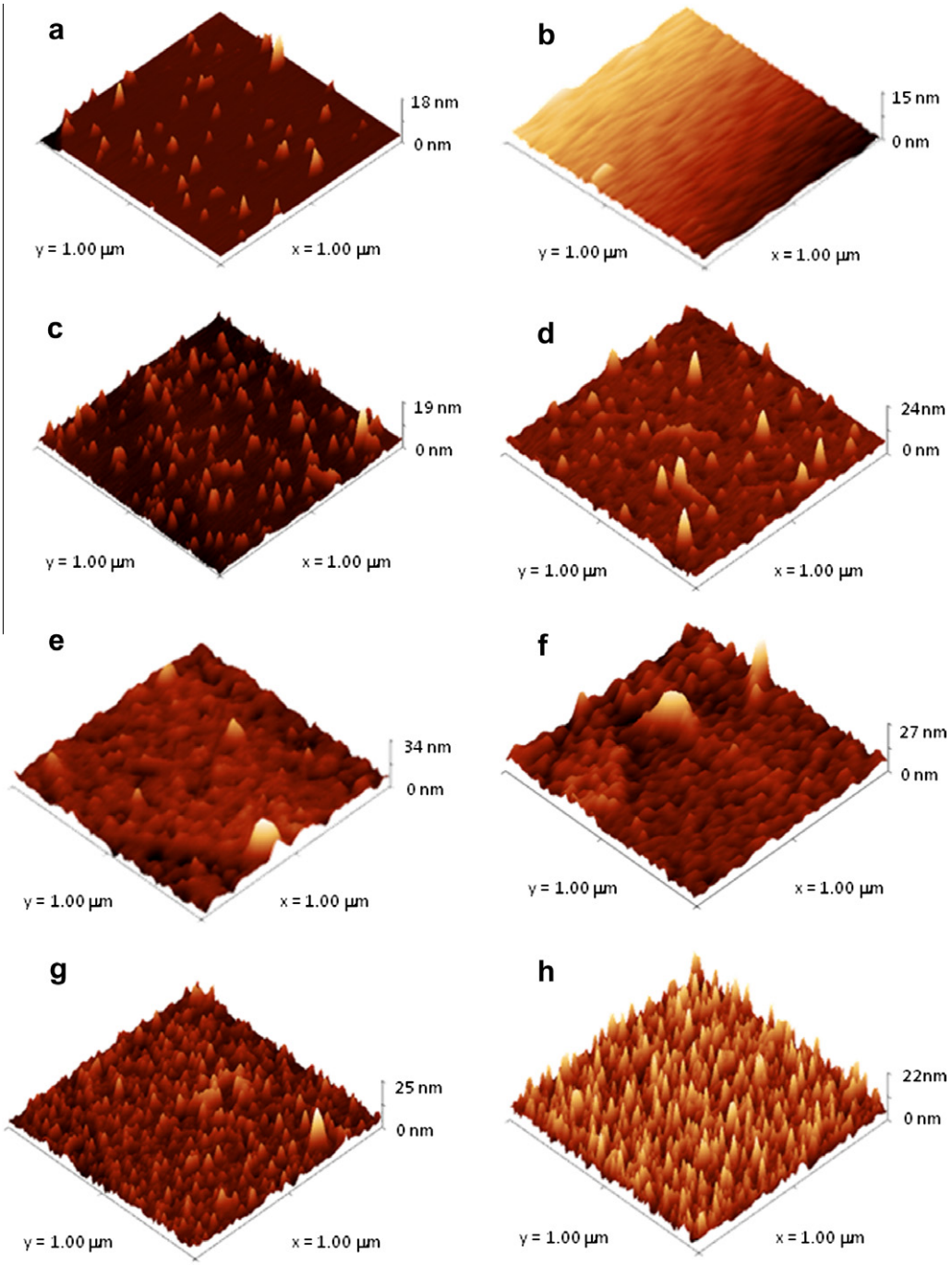

Fig. 2. An AFM topographic image (1.0 µm × 1.0 µm) of the HOPG surface modified with AuNp colloid (a), PVM layer (b), AuNpCys nanocomposite (c), PVM–AuNpCys–CramoLL–BSA (d), PVM–AuNpCys–CramoLL–BSA–*marcescens* (e), PVM–AuNpCys–CramoLL–BSA–*coli* (f), PVM–AuNpCys–CramoLL–BSA–*enterica* (g) and PVM–AuNpCys–CramoLL–BSA–*pneumoniae* (h).

3.3. Electrochemical impedance spectroscopy of PVM–AuNpCys–CramoLL–BSA on the electrode surface

The EIS measurements were performed in the presence of a redox probe $K_4[Fe(CN)_6]^{4-}/K_3[Fe(CN)_6]^{3-}$ in PBS buffer. Nyquist plots of impedance spectra of layer-by-layer self-assembled system are shown in Fig. S2 (see supporting information), a significant difference in the impedance spectra is observed on stepwise electrode modification and interaction between CramoLL and bacterial LPS.

Fig. S2 (see supporting information) shows the results of Faradaic impedance spectroscopy on the bare gold electrode (curve a), AuNpCys–modified gold electrode (curve b), AuNpCys–CramoLL–modified gold electrode (curve c), PVM–modified gold electrode (curve d), PVM–AuNpCys–CramoLL–modified gold electrode (curve e) and PVM–AuNpCys–CramoLL–BSA–modified gold electrode (curve f) in the presence of the $K_4[Fe(CN)_6]^{4-}/K_3[Fe(CN)_6]^{3-}$. It can be seen that the gold bare electrode exhibits an almost straight line that is characteristic of a diffusional limiting step in the electrochemical process. When the bare gold electrode was dipped into the AuNpCys colloidal solution, the EIS of the AuNpCys-modified electrode was similar to that of the bare gold electrode. The PVM molecules obstructed the charge transfer of the electrochemical probe and contributed to the increase in the

semicircle diameter (Fig. S2 in supporting information, curve d). After being modified with the PVM–AuNpCys–CramoLL system, the EIS of the PVM–AuNpCys–CramoLL-modified electrode shows a higher interfacial charge transfer resistance (R_{CT}) (Fig. S2 in supporting information, curve e). The impedance change in the modified process showed that the CramoLL lectin and PVM adhered to the gold electrode surface. When the PVM–AuNpCys–CramoLL–BSA was finally obtained, the interfacial resistance increased again, which indicated the formation of the sensor layer and the subsequent introduction of BSA hindering the electron transfer (Fig. S2 in supporting information, curve f).

In EIS, the impedance of the system was determined by some parameters, namely electrolyte resistance (R_Ω), constant phase element (Q), charge transfer resistance (R_{CT}), and Warburg element (W). The complex impedance can be presented by the relation between the real (Z') and imaginary (Z'') components that originate mainly from the resistance and capacitance of the electrochemical cell. The modified Randles equivalent circuit (see inset in Fig. 3) was chosen to fit the measured results. The R_Ω and W, represent bulk properties of the electrolyte solution and diffusion of the applied redox probe, respectively. The other two components of the circuit, Q and R_{CT}, depend on the dielectric and insulating features at the electrode/electrolyte interface. In EIS, the semicircle diameter of EIS equals the R_{CT}. In order to view the procedure of PVM–AuNpCys–CramoLL immobilization and amplified the lectin-carbohydrate interaction, we considered the relation between R_{CT} and the concentration of LPS from different bacterial LPS.

The impedance data were fitted with a Boukamp non-linear least square fitting program [27]. The fitting values for the stepwise formation of the biosystem are shown in Table 1. Starting from the bare gold electrode, the step-by-step modification is found to produce a significant increase in the charge transfer resistance together with a decrease in the double-layer capacitance, which confirms the good insulating properties of the system. In all the successive steps we found a systematic increase in R_{CT}, which indicates a blockage in the mass transfer phenomenon. The changes in R_{CT} were highly significant, compared with the other impedance components. The sequence of measurements AuNpCys–CramoLL, PVM–AuNpCys–CramoLL, and AuNpCys–PVM–CramoLL–BSA shows the additive blockage of the interface, confirming that the amount of material immobilized and/or adsorbed on the gold electrode surface directly correlates with the impedance.

It can be observed that, in general, the charge transfer resistances for the CramoLL system with LPS from *S. marcescens* are larger than those with other LPS tested from *E. coli*, *S. enterica* and *K. pneumoniae*, respectively (Fig. 3).

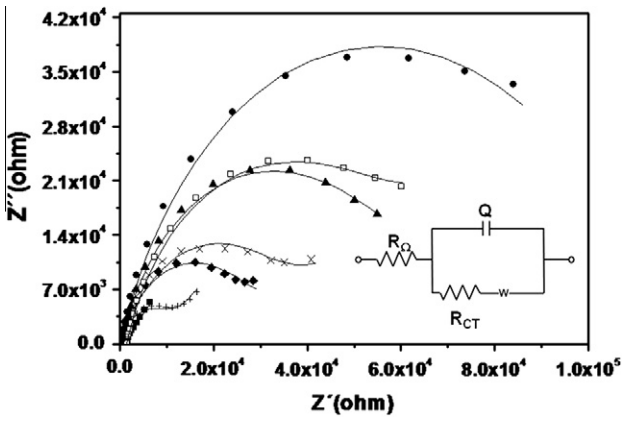

Fig. 3. Nyquist plot of the bare gold electrode (■), PVM–AuNpCys–CramoLL (+), PVM–AuNpCys–CramoLL–BSA (♦), PVM–AuNpCys–CramoLL–BSA–*pneumoniae* (×), PVM–AuNpCys–CramoLL–BSA–*enterica* (▲), PVM–AuNpCys–CramoLL–BSA–*coli* (□), and PVM–AuNpCys–CramoLL–BSA–*marcescens*, (●). Solid lines represent fitted data and scattered lines represent experimental data. Inset: modified Randles circuit.

Table 1
Values of the equivalent circuit elements from the fitted impedance result.

Modified electrode	RCT (kΩ)	Q (μF)	n
Bare gold electrode	2.11	7.76	0.68
AuNpCys	2.21	7.45	0.64
AuNpCys–CramoLL	3.02	7.00	0.85
PVM layer	6.18	7.10	0.80
PVM–AuNpCys–CramoLL	11.10	6.80	0.78
PVM–AuNpCys–CramoLL–BSA	29.10	7.20	0.76
PVM–AuNpCys–CramoLL–BSA–glucose	34.50	6.98	0.77
$CramoLL_{system}$–*coli* 200 μg/mL	69.10	5.21	0.78
$CramoLL_{system}$–*coli* 150 μg/mL	59.70	8.14	0.73
$CramoLL_{system}$–*coli* 100 μg/mL	40.70	8.84	0.68
$CramoLL_{system}$–*coli* 50 μg/mL	36.40	8.70	0.78
$CramoLL_{system}$–*coli* 25 μg/mL	31.00	6.47	0.75
$CramoLL_{system}$–glucose–*coli*[a]	35.47	6.45	0.74
$CramoLL_{system}$–*pneumoniae* 200 μg/mL	33.10	8.17	0.73
$CramoLL_{system}$–*pneumoniae* 150 μg/mL	32.40	8.14	0.70
$CramoLL_{system}$–*pneumoniae* 100 μg/mL	30.80	8.81	0.74
$CramoLL_{system}$–*pneumoniae* 50 μg/mL	30.67	7.79	0.73
$CramoLL_{system}$–*pneumoniae* 25 μg/mL	29.20	6.48	0.77
$CramoLL_{system}$–glucose–*pneumoniae*[a]	33.14	6.40	0.76
$CramoLL_{system}$–*enterica* 200 μg/mL	59.80	5.87	0.78
$CramoLL_{system}$–*enterica* 150 μg/mL	41.00	5.86	0.81
$CramoLL_{system}$–*enterica* 100 μg/mL	36.40	8.57	0.75
$CramoLL_{system}$–*enterica* 50 μg/mL	30.70	6.39	0.77
$CramoLL_{system}$–*enterica* 25 μg/mL	28.90	6.63	0.77
$CramoLL_{system}$–glucose–*enterica*[a]	34.78	6.60	0.76
$CramoLL_{system}$–*marcescens* 200 μg/mL	100.61	5.01	0.78
$CramoLL_{system}$–*marcescens* 150 μg/mL	61.70	8.53	0.74
$CramoLL_{system}$–*marcescens* 100 μg/mL	49.70	8.36	0.71
$CramoLL_{system}$–*marcescens* 50 μg/mL	43.10	5.45	0.76
$CramoLL_{system}$–*marcescens* 25 μg/mL	34.50	4.89	0.72
$CramoLL_{system}$–glucose–*marcescens*[a]	35.84	4.80	0.73

$CramoLL_{system}$ = PVM–AuNpCys–CramoLL–BSA.
[a] Assay with specific LPS at fixed concentration (200 μg/mL).

In addition, we used the monosaccharide glucose as a control to probe the lectin specificity to the LPS. After interaction between CramoLL and glucose our sensor did not recognize LPS molecules. From Table 1 we observed a small increase in R_{CT} associated with the PVM–AuNpCys–CramoLL–BSA system after interaction with monosaccharide glucose (R_{CT} = 34.4 kΩ). Otherwise, the PVM–AuNpCys–CramoLL–BSA–glucose system, after contact with LPS from *E. coli* (R_{CT} = 34.50 kΩ), *K. pneumoniae* (R_{CT} = 33.14 kΩ), *S. enterica* (R_{CT} = 34.74 kΩ) and *S. marcescens* (R_{CT} = 35.84 kΩ), showed an insignificant increase in the R_{CT}. Our results thus indicate that the LPS interacted specifically with the CramoLL binding sites, since there is no significant electrochemical response after blockage of the lectin-binding sites by glucose.

3.4. Sensitivity of the PVM–AuNpCys–CramoLL–BSA system to LPS

The impedance results shown in Fig. 3 may be interpreted in terms of the variation in the electron transfer resistance across the interface (ΔR_{CT}), according to the equation below:

$$\Delta R_{CT}\ (\%) = \frac{R_{CT}(\text{CramoLL—LPS}) - R_{CT}(\text{CramoLL})}{R_{CT}(\text{CramoLL})} \quad (1)$$

where R_{CT}(CramoLL) is the value of the electron transfer resistance of the PVM–AuNpCys–CramoLL–BSA-modified electrode before contact with lipopolysaccharide from different bacteria. R_{CT}(CramoLL–LPS) is the value of the electron transfer resistance of the PVM–AuNpCys–CramoLL–BSA-modified electrode after exposure to solutions containing LPSs from *E. coli*, *S. typhimurium*, *S. marcescens* and *K. pneumoniae*. A summary of these results is given in Table 2 for fixed LPS concentration (200 μg/mL). These results demonstrate that the lectin retained its capacity to recognize these glycoconjugates after adsorption.

Fig. 4 shows the effect of different concentrations of LPS from *E. coli*, *S. enterica*, *S. marcescens* and *K. pneumoniae* on ΔR_{CT} during the interaction of the lectin-modified electrode with glycoconjugates. In this case the electrode consisted of the PVM–AuNpCys–CramoLL–BSA and was used as the sensing basis for electrochemical impedance analyses of the CramoLL–lipopolysaccharide interaction. It can be seen that ΔR_{CT} is higher for *S. marcescens* and *E. coli* LPS than for *S. enterica* and *K. pneumoniae*, indicating that CramoLL was more specific to glycoconjugates present in LPS from *S. marcescens* and *E. coli*. Lectin from *Canavalia ensiformis* (ConA) exhibited a specific recognition of glycosyl residues present in lipopolysaccharide from *E. coli*, similar to that obtained for CramoLL lectin [28].

3.5. Properties of CramoLL lectin for LPS recognition

These results showed the bio-recognition process when the PVM–AuNpCys–CramoLL–BSA system interacted with the LPS tested. They demonstrate that this lectin retains its biological capability after exposition on the electrode surface. This behavior can be explained by the studies that were performed to determine the relevance of the neighborhoods of the monosaccharide-binding sites and accounts for the CramoLL response obtained for the bacterial LPS [20].

CramoLL lectin has important biological applications. It has been demonstrated that CramoLL binds to different glycoproteins present in human plasma [29] and shows differential binding to normal and transformed human mammary cells [30]. CramoLL exhibits high affinity for α-D-glucose, α-D-mannose, glycogen and glycoproteins [17]. This lectin recognizes monosaccharide and glycoprotein, which are the inhibitors of the agglutination of erythrocyte precipitation of carbohydrate polymers [17]. Recently, a number of authors [31,32] have demonstrated the ability of CramoLL to recognize epimastogote forms of *Trypanosoma cruzi* by means of the lectin interaction with glycoconjugates present in lipopeptidophosphoglycan from this cell.

Since the protein–carbohydrate interaction is a common phenomenon in biological systems, the study of the interactions between lectin and lipopolysaccharide has also been suggested for bacterial purification purposes, due to the ability of lectin to selectively bind cell wall oligosaccharides and to retain microbial cells in affinity chromatography that can be used to detect LPS in biological products administered intravenously, such as infusion fluids and injections [12,33,34]. Bacteria have chemically distinct surface polysaccharide carbohydrate structures that are recognized by CramoLL. Moreover, this lectin can bind to the carbohydrate moiety of glycoconjugates on the cellular membranes. This may be the reason why CramoLL has partial selectivity to the various LPS studied.

The CramoLL–bacterial LPS binding process may be related to the carbohydrates, glucose and mannose, imparting a LPS sensing mechanism on the CramoLL interface, a process similar to that observed for lectin ConA [35]. Experimental results demonstrate that the *S. marcescens* LPS interacts with the CramoLL system through the recognition of CramoLL with the glycosyl and mannosyl residues on the LPS structure. This may be related to the composition of LPS, since *S. marcescens* exhibit a linear polysaccharide composed of D-glucose-L-rhamnose disaccharide [7]. A structural study of *E. coli* K-235 LPS showed that the repetitive subunit sugar residues consist of glucosamine, galactosamine, glucose, galactose, rhamnose [9].

Although the CramoLL recognition of *S. enterica* and *E. coli* LPS was not as efficient as the response obtained for *S. marcescens*, it is probably associated with the presence of galactosyl residues in

Table 2
Relative charge transfer variation of the impedance data.

Condition	Before[a] ($CramoLL_{system}$)	After[b]	After[c]	After[d]	After[e]
R_{CT} (kΩ)	29.10	69.10	36.10	59.80	106.10
ΔR_{CT} (%)	–	137.45	13.74	105.49	264.60

$CramoLL_{system}$ = PVM–AuNpCys–CramoLL–BSA.
[a] Before contact with bacterial LPS.
[b] After contact with LPS from *E. coli*.
[c] After contact with LPS from *K. pneumoniae*.
[d] After contact with LPS from *S. enterica*.
[e] After contact with LPS from *S. marcescens*.

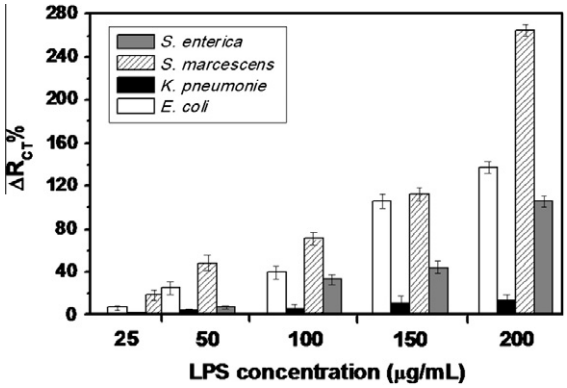

Fig. 4. ΔR_{CT}% for the systems that corresponded to the PVM–AuNpCys–CramoLL–BSA after interaction of *S. enterica*, *S. marcescens*, *K. pneumoniae* and *E. coli* at different concentrations (25 μg/mL, 50 μg/mL, 100 μg/mL, 150 μg/mL and 200 μg/mL).

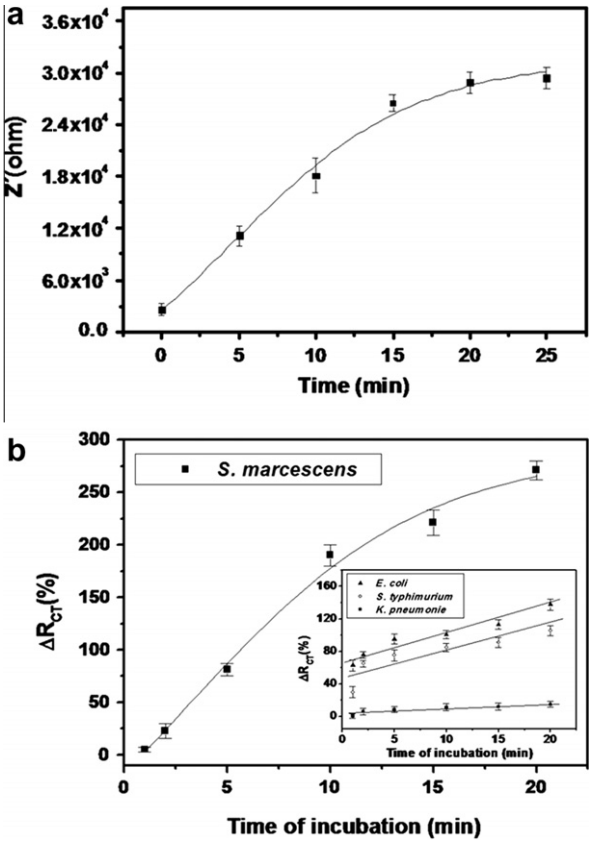

Fig. 5. ΔR_{CT} for the PVM–AuNpCys–CramoLL (a) and PVM–AuNpCys–CramoLL–BSA–LPS (b) for different interval times. Supporting electrolyte 10 mM $K_4[Fe(CN)_6]^{4-}/K_3[Fe(CN)_6]^{3-}$ 1:1 + 0.15 M NaCl in 10 mM pH 7.4 solution; frequency range at 100 mHz to 100 kHz.

Table 3
Amperometric anodic shift for the PVM–AuNpCys–CramoLL–BSA-modified electrode treated with 200 μg/mL bacterial LPS.

Condition	Before[a] (1/*I*b, μA^{-1})	After[b] (1/*I*a, μA^{-1})	After[c] (1/*I*a, μA^{-1})	After[d] (1/*I*a, μA^{-1})	After[e] (1/*I*a, μA^{-1})
$CramoLL_{system}$	0.289	0.335	0.840	0.549	0.292
ΔI (%)	–	15.91	190.7	89.96	1.02

$CramoLL_{system}$ = PVM–AuNpCys–CramoLL–BSA.
[a] Before contact with bacterial LPS.
[b] After contact with LPS from *S. enterica*.
[c] After contact with LPS from *S. marcescens*.
[d] After contact with LPS from *E. coli*.
[e] After contact with LPS from *K. pneumoniae*.

these structures. Studies have shown that O-antigens of *S. enterica* contain around 20 repeats of a common main-chain trisaccharide unit consisting of D-mannose, L-rhamnose and D-galactose [11]. *Klebsiella* O antigens basically consist of homopolymers of galactose. The O polysaccharide is composed of two discrete repeat-unit structures of D-galactan [4,5]. The CramoLL response to *K. pneumoniae* LPS showed a distinct result that is related to the composition of O polysaccharide composed of galactose. This variable may influence in the CramoLL biological activity in the recognition of the corresponding endotoxin.

3.6. Reproducibility

Reproducibility of the biosensor system was evaluated from the highest ΔR_{CT} response for each LPS (concentration of 200 μg/mL) at different nanobiosensors, and acceptable R.S.D. values of 5.78%, 5.25%, 5.71% and 4.89% for *S. marcescens*, *E. coli*, *S. enterica* and *K. pneumoniae*, respectively, were observed. These results indicate the suitability of the PVM–AuNpCys–CramoLL–BSA–modified nanobiosensor for practical applications.

3.7. The effects of the incubation time for PVM–AuNpCys–CramoLL–BSA system and bacterial LPS interaction

The influence of the incubation period was investigated to evaluate PVM–AuNpCys–CramoLL–BSA adsorption and to improve the sensitivity of the biosensor response. The PVM–AuNpCys–CramoLL–BSA system was evaluated at 5–25 min (Fig. 5a) and this assay revealed a saturation behavior at the highest tested time. The time chosen was 5 min to evaluate the subsequent steps of surface modification. LPS solutions from *K. pneumoniae*, *S. enterica*, *E. coli* and *S. marcescens* (200 μg/mL; pH 7.4, PBS) were placed on the surface of PVM–AuNpCys–CramoLL–BSA-modified electrode for different time periods ranging from 2 to 20 min. The time chosen was evaluated by monitoring the change in R_{CT} using $K_4[Fe(CN)_6]^{4-}$/$K_3[Fe(CN)_6]^{3-}$ as redox probes. The results indicated that the incubation time allows an improvement in the interaction between adsorbed CramoLL lectin and LPS and amplifies their interaction with a tendency to saturation for *S. marcescens* and linear behavior for *K. pneumoniae*, *E. coli* and *S. enterica* (Fig. 5b). Thus, 20 min was chosen as the optimized recognition time.

3.8. Electrochemistry characteristics of the PVM–AuNpCys–CramoLL–BSA system by cyclic voltammetry

In the presence of a fairly reversible redox couple $K_4[Fe(CN)_6]^{4-}$/$K_3[Fe(CN)_6]^{3-}$, CV was used to monitor the electrode modification. As shown in Fig. S3 (see supporting information), the pretreated bare gold electrode produces a reversible cyclic voltammogram (curve a). After electrode modification with AuNpCys (curve b) and AuNpCys–CramoLL (curve c), a small decrease in the amperometric response was obtained. The formation of the PVM–AuNpCys–CramoLL system on the gold electrode is accompanied by a considerable decrease in the amperometric response of the electrode and an increase in the peak-to-peak separation of the cathodic and anodic waves of the redox probe (curve d). This confirms that the electrode modification with CramoLL and PVM resulted in an insulating surface and the electron transfer kinetics of $K_4[Fe(CN)_6]^{4-}$/$K_3[Fe(CN)_6]^{3-}$ are disrupted.

Following the blockage of the free space inside the modified gold electrode with BSA, a new decrease in the response of the current is observed (curve f). Furthermore the CramoLL biological activity in the PVM–AuNpCys–CramoLL–BSA system was demonstrated. Curves e and g exhibit the CV responses after the CramoLL response to LPS from *K. pneumoniae* and *S. enterica*, respectively. However, a good response was obtained for *E. coli* (curve h) and *S. marcescens* (curve i), which reflects a specific CramoLL interaction to complex carbohydrates such as bacterial LPS. In particular, after LPS from *S. marcescens* were coupled onto the CramoLL molecules, there was a considerable increase in peak separation and an almost total disappearance of the peak shape was observed. Since the adsorption of species decreases the current, an analysis analogous to the one carried out for the impedance results can be compared with the peak currents. The extent of adsorption may be expressed in the following relative percentage deviation:

$$\Delta I\ (\%) = \frac{[(1/Ib) - (1/Ia)]}{(1/Ib)} \times 100 \qquad (2)$$

where *I*b is the anodic peak current before binding the lectin with LPS and *I*a is the anodic peak current after the LPS interaction. Table 3 shows the results of this analysis for the PVM–AuNpCys–CramoLL–BSA-modified electrode before and after the reaction to 200 μg/mL of bacterial LPS tested. All the measurements were repeated three times and the results were almost the same.

The PVM–AuNpCys–CramoLL system can be used to detect LPS from bacteria with glycosyl residues and these cellular products are involved for public health. Since LPS triggers a wide variety of biological effects in human, such as septic shock and coagulopathies, its detection is mandatory.

4. Conclusions

In the present work, a new strategy aimed at constructing an electrochemical biosensor for bacterial lipopolysaccharides based on a PVM–AuNpCys–CramoLL–BSA-modified electrode has been proposed. The biosensor described here has a good accuracy, stability, and reproducibility. In addition, the CramoLL–LPS binding process can be significantly inhibited by saccharide, glucose, providing further proof of the sensing mechanism on the lectin interface. The AuNpCys–PVM positively-charged surfaces were suitable for CramoLL lectin immobilization. By this means we were able to observe that CramoLL retained its biological activities after contact with the electrode surface. CV and EIS were applied to evaluate the detection of LPS in the presence of the $K_4[Fe(CN)_6]^{4-}$/$K_3[Fe(CN)_6]^{3-}$ redox probe. CramoLL interacted selectively with LPS from *S. marcescens*, *E. coli*, *S. enterica* and *K. pneumoniae*, thereby demonstrat-

ing that the CramoLL system can be used to detect the presence of complex glycoconjugates. The PVM–AuNpCys–CramoLL–BSA system provides an appropriate biomimetic interface for the specific recognition of bacterial LPS.

Acknowledgments

Drs. Andrade and Oliveira are grateful for the support provided by the Rede ELINOR de Nanobiotecnologia/Coordenação de Aperfeiçoamento de Pessoal de Nível Superior (CAPES). CASA would like to thank CAPES for a postdoctoral Grant (BEX 3561/10-0).

Appendix A. Supplementary material

Supplementary data associated with this article can be found, in the online version, at doi:10.1016/j.jcis.2011.06.042.

References

[1] A. Preston, R.E. Mandrell, B.W. Gibson, M.A. Apicella, Crit. Rev. Microbiol. 22 (1996) 139.
[2] C. Alexander, E.T. Rietschel, J. Endotoxin Res. 7 (2001) 167.
[3] E. Vinogradov, M.B. Perry, Carbohydr. Res. 335 (2001) 291.
[4] C. Whitfield, J.C. Richards, M.B. Perry, B.R. Clarke, L.L. MacLean, J. Bacteriol. 173 (1991) 1420.
[5] O. Kol, J.-M. Wieruszeski, G. Strecker, J. Montreuil, B. Fournet, Carbohydr. Res. 217 (1991) 117.
[6] C.L. Kurz, S. Chauvet, E. Andres, M. Aurouze, I. Vallet, G.P. Michel, M. Uh, J. Celli, A. Filloux, S. De Bentzmann, I. Steinmetz, J.A. Hoffmann, B.B. Finlay, J.P. Gorvel, D. Ferrandon, J.J. Ewbank, EMBO J. 22 (2003) 1451.
[7] C.S. Wang, P. Alaupovic, Biochemistry 12 (1973) 309.
[8] K.L. Vosti, J. Infect. 55 (2007) 8.
[9] F.C. McIntire, H.W. Sievert, G.H. Barlow, R.A. Finley, A.Y. Lee, Biochemistry 6 (1967) 2363.
[10] R.K. Beal, P. Wigley, C. Powers, S.D. Hulme, P.A. Barrow, A.L. Smith, Vet. Immunol. Immunopathol. 100 (2004) 151.
[11] M. Devyatyarova-Johnson, I.H. Rees, B.D. Robertson, M.W. Turner, N.J. Klein, D.L. Jack, Infect. Immun. 68 (2000) 3894.
[12] J.M. Ahn, P. Wentworth, K.D. Janda, Chem. Comm. 4 (2004) 364.
[13] D. Kato, S. Iijima, R. Kurita, Y. Sato, J.B. Jia, S. Yabuki, F. Mizutani, O. Niwa, Biosens. Bioelectron. 22 (2007) 1527.
[14] A. Hreniak, K. Maruszewski, J. Rybka, A. Gamian, J. Czyzewski, Opt. Mater 26 (2004) 141.
[15] E.A. James, K. Schmeltzer, F.S. Ligler, Appl. Biochem. Biotechnol. 60 (1996) 189.
[16] M. Yang, J. Chen, Anal. Lett. 35 (2002) 1775.
[17] M.T.S. Correia, L.C.B.B. Coelho, Appl. Biochem. Biotechnol. 55 (1995) 261.
[18] N. Sharon, Trends Biochem. Sci. 18 (1993) 221.
[19] C.A.S. Andrade, M.T.S. Correia, L.C.B.B. Coelho, S.C. Nascimento, N.S. Santos-Magalhaes, Int. J. Pharm. 278 (2004) 435.
[20] G.A. de Souza, P.S.L. Oliveira, S. Trapani, A.C.O. Santos, J.C. Rosa, H.J. Laure, V.M. Faça, M.T.S. Correia, G.A. Tavares, G. Oliva, L.C.B.B. Coelho, L.J. Greene, Glycobiology 13 (2003) 961.
[21] X. Li, J. Wu, N. Gao, G. Shen, R. Yu, Sens. Actuators, B 117 (2006) 35.
[22] D.M.N. Luna, E.P.S. Falcao, S.J. Melo, C.A.S. Andrade, Colloids Surf., A 373 (2011) 22.
[23] M.D.L. Oliveira, C.P. de Melo, O. Glaucius, C.A.S. Andrade, Colloids Surf., B 82 (2011) 365.
[24] M.D.L. Oliveira, M.T.S. Correia, F.B. Diniz, Biosens. Bioelectron. 25 (2009) 728.
[25] S. Aryal, B.K.C. Remant, N. Dharmaraj, N. Bhattarai, C.H. Kim, H.Y. Kim, Spectrochim. Acta Part A 63 (2006) 160.
[26] J. Strauss, N.A. Burnham, T.A. Camesano, J. Mol. Recognit. 22 (2009) 347.
[27] B.A. Boukamp, Solid State Ionics 18–19 (1986) 136.
[28] P. Ertl, S.R. Mikkelsen, Anal. Chem. 73 (2001) 4241.
[29] V.L.M. Lima, M.T.S. Correia, Y.M.N. Cechinel, C.A.M. Sampaio, J.S. Owen, L.C.B.B. Coelho, Carbohydr. Polym. 33 (1997) 27.
[30] E.I.C. Beltrao, M.T.S. Correia, J. Figueredo-Silva, L.C.B.B. Coelho, Appl. Biochem. Biotechnol. 74 (1998) 125.
[31] N. Varejao, M.D. Almeida, N.N.T. De Cicco, G.C. Atella, L.C.B.B. Coelho, M.T.S. Correia, D. Foguel, Biochim. Biophys. Acta 1804 (2010) 1917.
[32] M.P. Fernandes, N.M. Inada, M.R. Chiaratti, F.F.B. Araujo, F.V. Meirelles, M.T.S. Correia, L.C.B.B. Coelho, M.J.M. Alves, F.R. Gadelha, A.E. Vercesi, J. Bioenerg. Biomembr. 42 (2010) 69.
[33] D. Mirelman, I. Ofek, Microbial Lectins and Agglutinins, Properties and Biological Activity, in: D. Mirelman (Ed.), John Wiley & Sons, New York, 1986.
[34] H. Lis, N. Sharon, Chem. Rev. 98 (1998) 637.
[35] F. Xi, J. Gao, J. Wang, Z. Wang, J. Electroanal. Chem. 656 (2011) 252.